was omitted in arriving at Eq. (5). This was advertently neglected in view of the inequality $\omega^2\tau_0^2 \gg 1$, and assuming the sample length to be small. Moreover, it has been demonstrated earlier by Sodha *et al.*[9] that inclusion of absorption, unless very high, only slightly affects the self-focusing length (for a positive coefficient of absorption, it results in increase) and primarily changes the field pattern inside the sample, which is not relevant to us here. Thirdly, besides a linear absorption term there is a part contained in Eq. (4) which corresponds to nonlinear absorption, quadratic in field. This gives rise to interesting effects such as those discussed in Ref. 3. Essentially, inclusion of nonlinear absorption results in increase of self-focusing length. We had neglected this part also. However, if one wishes to take account of absorption for long samples, calculations can be made proceeding with Eq. (4) by evaluating the real part of the oscillatory current.

We finally conclude that the EDS mechanism outlined in this paper may contribute significantly to the self-focusing phenomenon of laser beams in semiconductors.

---

*Partly supported by the National Research Council of Canada.

[1] N. Tzoar and J. I. Gersten, Phys. Rev. Letters 26, 1634 (1971).

[2] N. Tzoar and J. I. Gersten, Phys. Rev. B 4, 3540 (1971).

[3] For an excellent review of general theoretical and experimental aspects of the phenomenon, see the review by S. A. Akhmanov, A. P. Sukhorukov, and R. V. Khokhlov, Usp. Fiz. Nauk 93, 19 (1968) [Sov. Phys. Usp. 10, 609 (1968)]; also, see Zh. Eksperim. i Teor. Fiz. 50, 1537 (1966) [Sov. Phys. JETP 23, 1025 (1966)].

[4] E. L. Kerr, IEEE J. Quantum Electron. QE-6, 616 (1970).

[5] Ya. B. Zeldovich and Yu. P. Raizer, Zh. Eksperim. i Teor. Fiz. Pis'ma v Redaktsiyu 3, 137 (1966) [Sov. Phys. JETP Letters 3, 86 (1966)]; Y. R. Shen, Phys. Letters 20, 378 (1966).

[6] C. Wang, Phys. Rev 173, 908 (1968); R. Y. Chiao, E. Garmire and C. H. Townes, Phys. Rev. Letters 13, 479 (1964); 14, 1056 (1965).

[7] F. G. Gebhardt and D. C. Smith, IEEE J. Quantum Electron. QE-6, 63 (1971).

[8] If one also includes nonparabolicity, we may point out that *n* is equal to 4 rather than 3.

[9] M. S. Sodha, D. P. Tewari, Jyoti Kamal, and V. K. Tripathi (unpublished).

PHYSICAL REVIEW B VOLUME 6, NUMBER 4 15 AUGUST 1972

Study of V_2O_3 by X-Ray Photoelectron Spectroscopy

J. M. Honig* and L. L. Van Zandt*
Department of Chemistry and Physics, Purdue University, West Lafayette, Indiana 47907

and

R. D. Board and H. E. Weaver
Scientific Instruments Division, Hewlett Packard Company, Palo Alto, California 94304

(Received 27 March 1972)

The band structure of V_2O_3 below the Fermi level has been studied by x-ray photoelectron spectroscopy both above and below the Néel temperature. Aside from normal bands associated with atomic states from 20 to 640 eV, a valence band with structure was observed in the range 0–10 eV. The results are compared to soft-x-ray-emission and -absorption results and to theoretical predictions concerning the band structure of V_2O_3.

I. INTRODUCTION

We report in this paper on the band structure of V_2O_3 below the Fermi level, as determined by x-ray photoelectron spectroscopy (commonly termed ESCA). Early applications of this technique have been reviewed by Siegbahn and co-workers[1]; additional studies have been reported for metals,[2,3] semiconductors,[4] and near insulators.[5–7] As far as we are aware, the technique has not been applied to materials which undergo a semiconductor-metal transition, such as V_2O_3. At 170 K this compound exhibits sharp changes in physical properties as a concomitant to alterations in magnetic and crystallographic properties. These matters are reviewed elsewhere.[8–11]

II. EXPERIMENTAL

The investigations were carried out with a Hewlett-Packard model No. 5950 A spectrometer with provision for dispersion compensation. Monochromatic Al$K\alpha_{1,2}$ radiation was obtained from a quartz-crystal disperser at high Bragg angle. Electrons, which are ejected by the interaction of the radiation with the sample, are focused on the entrance of an electron spectrometer and emerge after having passed through the hemispherical energy analyzer. The resulting spectrum was free of spurious line broadening, extraneous satellites, and interference from bremsstrahlung radiation.

Investigations were carried out on two single crystals, on powders dispersed on gold or on cellophane tape, and on powder imbedded in graphite; results obtained with various specimens are in substantial agreement. In what follows, all binding energies are referred to the Fermi level of gold, which was repeatedly used as a fiducial marker.

Before discussing the results it is necessary to point out several distracting complications that contribute to uncertainties in the interpretation of the data: (a) A large fraction of the photoelectrons originate from surface regions of the sample. Estimates in the literature of the depth of the emission region range from 4 to 100 Å. At best, one encounters a superposition of spectra associated with the bulk and surface regions. If the corresponding electron states are of different energy, then the bulk spectrum will be broadened or distorted. At worst, one observes only energies associated with electrons in surface regions. It appears virtually impossible to eliminate problems of this nature. (b) Certain impurities, especially when aggregated on the surface, contribute their own spectra, and may interfere seriously with the analysis of spectra in the valence-band region, roughly from 0 to 10 eV. The powder used in the present study had an average total impurity content of 50 ppm, whereas that of the single crystal was in the range of 100 ppm. It is unlikely that impurities in this concentration range invalidate the results in Sec. III, but they could well be the cause of small, apparently extraneous, peaks in some of the observed spectra. (c) Frequently one encounters in insulators a charging effect, i.e., a shift of spectra to higher binding energies due to uncompensated holes generated during the photoemission process. In highly insulating samples these holes are not all neutralized. However, this does not appear to have been a major problem in the present measurements, since the positions of all peaks in eleven sets of experiments on five samples were generally reproducible to ± 0.3 eV. In particular, there was no significant change in peak position in passing from the metallic to the insulating phase, where charging effects are likely to be more serious. (d) Some of the peak width, particularly in the range of higher binding energies, is ascribable to line broadening associated with the short lifetime of excited states. The instrumental resolution of 0.3 eV also contributed to peak broadening. However, these effects are of lesser importance in the range of binding energies near the Fermi level, where the bands are intrinsically broad; this is the region of greatest interest. (e) Peak heights must be interpreted in terms of quantum-mechanical transition probabilities from the electron state in the crystal to the free state of the photoejected electron. The transition probabilities vary with different bands which therefore develop at different rates; there is no simple correlation between peak heights and densities of states. This matter is referred to elsewhere[12] in greater detail; it also figures prominently in any attempts to develop weak peaks, because of the $t^{1/2}$ factor in the time required to improve the signal to noise ratio. (f) The edges of the peaks were rather fuzzy, making an assignment of bandwidths uncertain. Standard triangulation techniques were used to locate the edges in complex spectra.

III. RESULTS

Figure 1 shows the elemental levels of V and of O as cited by Bearden and Burr[13]; the corresponding electronic energy states in V_2O_3 are also shown. The hatched regions indicate roughly the half-widths of the observed peaks. It is seen that there is a one-to-one correspondence between atomic and band states. The proximity of peak positions on the energy scale to the values cited in Ref. 13 was used as a basis for identifying the bands; it must be remembered, however, that these latter values refer to elemental states and

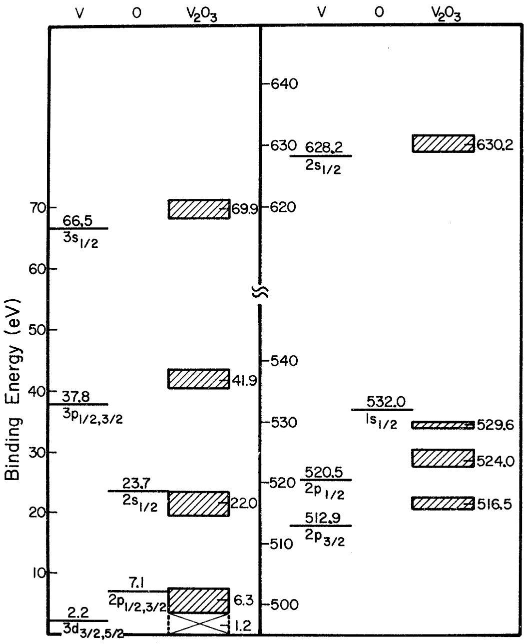

FIG. 1. Summary of binding energies for V, O, as cited in Ref. 13, and of bands (relative to the Fermi level of gold) in V_2O_3, as determined by x-ray photoelectron spectroscopy.

are based on their own appropriate Fermi levels, whereas our results pertain to the V_2O_3 compound and are referred to the Fermi level of gold. Undoubtedly, line broadening due to instrumental resolution, short lifetimes of the excited states, as well as surface inhomogeneities, contribute to the peak half-widths of the low-lying states. These were of the order of 1.5 eV for the band derived from the O 1*s* state and in the range of 2 to 3 eV for bands derived from the V 2*s* and 2*p* states. The three bands in the range 20–72 eV are characterized by half-widths slightly in excess of 3 eV. When specimens were cooled to 77 K or severely abraded, extra O 1*s* lines of smaller intensity appeared in the energy range 531–534 eV, showing that absorbed water or severe disordering on the surface may be detected in this manner.

The bands associated with O 2*s*, V 2*s*, and V 3*s* states were found to be symmetric, as was the V 3*p* band, where an incipient splitting into V $3p_{1/2}$ and V $3p_{3/2}$ substates might have been anticipated. Figure 2 shows a smoothed scan of the 540–495-eV region for the O $1s_{1/2}$, V $2p_{1/2}$, and V $2p_{3/2}$ bands. Our results differ in some respects from those cited by Fischer,[14] who investigated the emission and absorption spectra of V_2O_3 using x-ray radiation in the 23.5–25.5-Å region. To establish a basis for comparison we show in Table I a set of transition energies anticipated in the range 485–535 eV. The first column was calculated from the tabulation by Bearden and Burr[13] for elemental atomic-energy states; one would not necessarily anticipate good agreement with measured values in the compound. In the second column are listed the transition energies as determined by Fischer from soft-x-ray-emission and -absorption lines. The transition energies as computed from the data in Fig. 1 are shown in the last column. In rare instances the latter sets of figures agree; however, discrepancies of up to 10 eV are encountered. These may be traced to several sources: In several cases it is difficult to estimate the peak positions in Fischer's x-ray spectra, particularly where shoulders or small peaks are involved. Furthermore, the process of photoemission differs physically from photoexcitation where the promoted electron remains initially within the crystal. In the former case there is a regrouping of electrons in the energy states contiguous to those from which the photoelectron originated. In the latter, such rearrangements occur both for the initial and for the final energy states. Thus, there are concomitant differences in electronic rearrangement energies that could well amount to several electron volts. That such a factor might play a role is also made plausible by comparing the L_3-absorption-band edge of 512.7 ± 0.3 eV as reported by Fischer with the value of 516.5 eV obtained in our work. Here one presumably compares the transition of an electron from the V $2p_{3/2}$ state to the Fermi level of V_2O_3 (x-ray transition) with the position of the V $2p_{3/2}$ state relative to the Fermi level of gold (x-ray photoejection). The 3.8-eV discrepancy presumably measures the magnitude of the rearrangement energy. Incidentally, whereas the work function of V_2O_3 is not known, that of the related VO_2 is 4.5 eV.[15] This compares to the range of 4.00 to 6.24 eV in Au.[16] It must be concluded that internal rearrangement energies play an important role and that they should be taken into account in any comparison of the type attempted here. For more conclusive evidence regarding the same phenomenon in other materials the reader is referred to other sources.[6,17]

TABLE I. Comparison of transition energies in the 405–538-eV range based on various sources.

Type of transition	Energy change in eV Bearden and Burr (Ref. 13)	Fischer (Ref. 14)	Present results
V $M_{4,5} \rightarrow$ O K	529.8	531[a]	528.4
O $L_{2,3} \rightarrow$ O K	524.9	525	523.3
O $L_1 \rightarrow$ O K	508.3	···	507.6
V $M_{2,3} \rightarrow$ O K	494.2	497.8	487.7
V $M_{4,5} \rightarrow$ V L_2	517.3	519	522.8
O $L_{2,3} \rightarrow$ V L_2	513.4	514	517.7
O $L_1 \rightarrow$ V L_2	496.8	502	502.0
V $M_{2,3} \rightarrow$ V L_2	482.7	···	482.1
V $M_{4,5} \rightarrow$ V L_3	510.7	512.3	515.3
O $L_{2,3} \rightarrow$ V L_3	505.8	508.5	510.2
O $L_1 \rightarrow$ V L_3	489.2	491.2	494.5

[a] Unlabeled major peak, tentatively assigned by us to this transition.

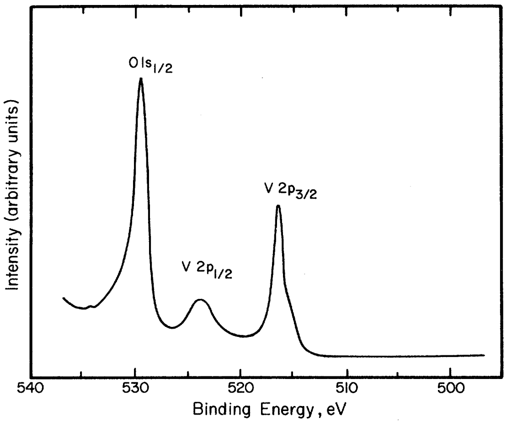

FIG. 2. X-ray photoelectron spectra in V_2O_3 powder in the range 500–540 eV relative to the Fermi level of gold (smoothed experimental data).

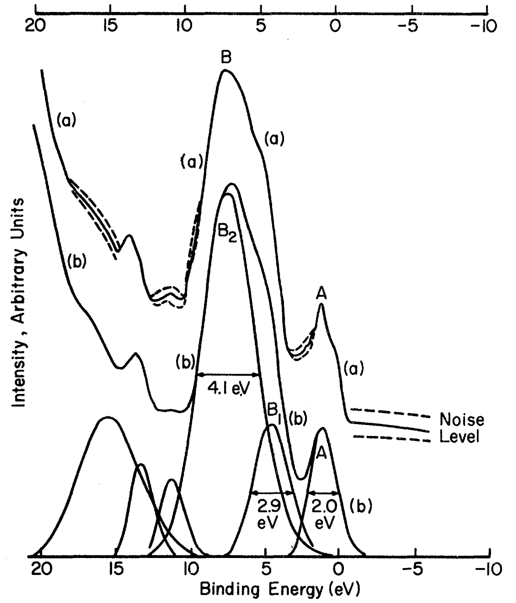

FIG. 3. X-ray photoelectron spectra in a single crystal of V_2O_3 in the range 0–20 eV relative to the Fermi level of gold. (a) Original data with noise level indicated by dashed lines; (b) smoothed data with computer resolution into component Gaussian peaks.

Spectra obtained in the 0–20-eV range are represented by Fig. 3(a), which was obtained at 300 K over a 13-h period. The small peak immediately to the left of the 0-eV fiducial marker is barely visible for an exposure time of 5 h, and it disappears under the noise for exposure times of 4 h or less. However, its presence may be inferred indirectly, in these circumstances, by the abrupt rise in the base line for the region 0 to +2.5 eV, relative to the position of the base line for the 0–2.5-eV range. The peak under discussion also failed to develop in all measurements at liquid-nitrogen temperatures which necessarily were limited to short exposures and complicated by the absorption of moisture which slowed down the development of the V_2O_3 peaks at 78 K. In all cases where the peak was not observed the base-line shift referred to earlier was found.

The small peak centered about 14 eV was not encountered in any of the other twelve measurements made on various V_2O_3 specimens over periods ranging from 0.5 to 6 h. We therefore tentatively attribute this peak to an impurity. The sharp shoulder starting at 15 eV is part of the O 2*s* peak centered about 22 eV.

In Fig. 3(b) is shown the computer resolution of the smoothed spectra into Gaussian-type component curves. We focus attention only on the Gaussian peaks labeled *A*, B_1, and B_2. If the spectra lying between 10 and 632 eV have been correctly accounted for, then the spectral peaks labeled *A* and *B* in Fig. 3(a) or the three components *A*, B_1, and B_2 in Fig. 3(b) must be correlated with the remaining bands of primarily anionic 2*p* character and of primarily cationic 3*d* character. This correlation may be done in two ways: (a) One may associate the large peak *B* containing components B_1 and B_2 with the O 2*p*-type band, in which event

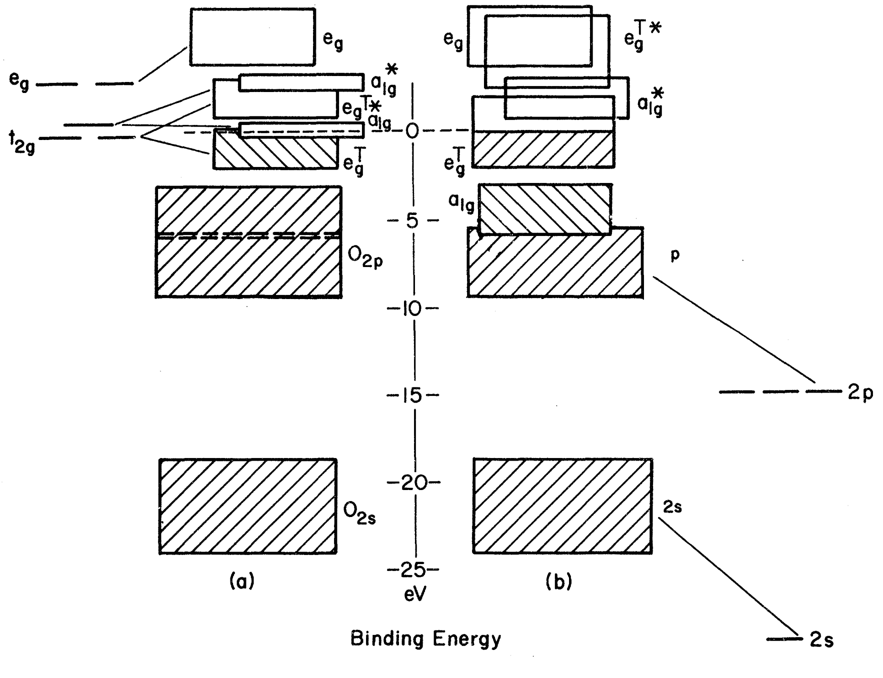

FIG. 4. Schematic band structure diagram for bands of primarily O 2*s*, O 2*p*, and V 3*d* character. (a) Diagram according to Goodenough (Ref. 10); (b) diagram with e_g^T and a_{1g} bands inverted on the energy scale.

the remaining peak A is related to the density of states of the occupied portion of the V $3d$-type band. The two portions B_1 and B_2 in Fig. 3(b) would then be quite plausibly interpreted as due to a partial splitting of p-like states into e- and a-type subbands in the rhombohedral field of the lattice. Peak A then represents the $e_g^T - a_{1g}$ states of of the $3d$ bands, as is made more explicit in Fig. 4(a) which is based on a qualitative band structure diagram proposed by Goodenough.[10] The diagram is consistent with the experimental observation that the c/a ratio of lattice parameters in V_2O_3 is unusually high in the sesquioxides with corundum structure. The almost complete filling of the e_g^T states with electrons and the fractional filling of a_{1g} states imply a heavy electron concentration in bonds lying primarily in the basal plane and of sparse electron occupancy of bonds with lobes largely parallel to the c axis. In this interpretation the $e_g^T - a_{1g}$ peak labeled A has a combined width of 2.0 eV, and the O $2p$-like band, a combined width of 6.9 eV. (b) Alternatively, one may associate the Gaussian peak B_2 with the O $2p$-type band which would then have a width of 4.1 eV. In this alternative, peaks A and B_1 would have to represent two portions of the cationic d-like band with widths of 2.9 and 2.0 eV, respectively. This assignment is compatible, but only in zero-order approximation, with *a priori* calculations of the band structure and with the densities-of-states curve for V_2O_3 published by Nebenzahl and Weger.[18] Their density-of-states curve is reproduced in Fig. 5. While this calculation predicts a rather sharp dip for the density-of-states curve, the total computed width of the occupied portion as obtained in Ref. 18 is only 1.5 eV, as against a combined width of about 5 eV for peaks A and B_1 in Fig. 3. Moreover, such an assignment requires an inversion of the a_{1g} and e_g bands on the energy scale, as depicted in Fig. 4(b), which is not as compatible with the large c/a ratio as is the alternative described earlier. For these reasons we regard alternative (a) as the more likely correlation.

It is important to note that none of the spectra in the 3–632 eV range is altered significantly in passing from room temperature to liquid-nitrogen temperature. This indicates that in undergoing the semiconductor-metal transition the various bands in V_2O_3 shift by less than 0.3 eV. As stated earlier, the one possible exception is the d-like peak which is not evident in any spectra of the low-temperature phase. We have verified, however, that the noise level was sufficiently large in all such cases to have masked a d-like peak of the anticipated size. Furthermore, the alteration in baseline characteristics for energies immediately above and below 0 eV makes it plausible that this particular peak is in fact present in the spectra of the insulating phase.

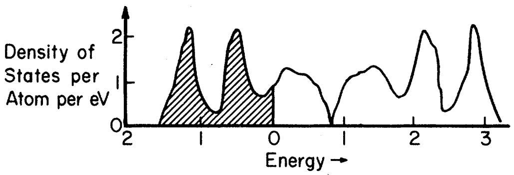

FIG. 5. Schematic representation of density-of-states calculations by Nebenzahl and Weger (Ref. 18).

In conjunction with the Mott transition model that has been postulated[8] to explain the semiconductor-metal transition in V_2O_3, it is of interest to search for the existence of localized states in the V_2O_3 spectrum taken at 78 K; for, such states must be present if the model is to have any validity. Localized states might be made manifest by the presence of spikes in the spectra. Our failure to observe such peaks under the prevailing experimental conditions leaves the question of their presence open until such time as the instrumental resolution is considerably improved.

ACKNOWLEDGMENTS

One of us (J.M.H.) wishes to thank the staff of the Hewlett-Packard Scientific Instruments Division for their generous hospitality during the time that the above research was carried out. The authors are indebted to Dr. A. Melera of Hewlett-Packard Co. for assistance and to George Yuochunas of Purdue University for growing the single crystals. They acknowledge stimulating conversations with Professor J. W. Richardson.

---

[*] Work supported in part under Grant No. DAHC 15 69C 0213 at the ARPA-IDL Program at Purdue University.

[1] K. Siegbahn, C. Nordling, A. Fahlman, R. Nordberg, K. Hamrin, J. Hedman, G. Johannson, T. Bergmark, S. E. Karlsson, I. Lindgren, and B. Lindberg, in *ESCA-Atomic, Molecular, and Solid State Structure Studied by Means of Electron Spectroscopy* (North-Holland, Amsterdam, 1967).

[2] C. S. Fadley and D. A. Shirley, Phys. Rev. Letters 21, 980 (1968).

[3] Y. Baer, P. F. Heden, M. Klasson, C. Nordling, and K. Siegbahn, Solid State Commun. 8, 517 (1970).

[4] D. W. Langer, Z. Naturforsch. 24a, 1555 (1969).

[5] L. Ramqvist, K. Hamrin, G. Johannson, A. Fahlman, and C. Nordling, J. Phys. Chem. Solids 30, 1835 (1969).

[6] T. Novakov, Phys. Rev. B 3, 2693 (1971).

[7] L. Ramqvist, K. Hamrin, G. Johansson, U. Gelius, and C. Nordling, J. Phys. Chem. Solids 31, 2669 (1970).

[8] D. B. McWhan and J. P. Remeika, Phys. Rev. B 2, 3734 (1970), and subsequent papers in the same issue.

[9] T. M. Rice and D. B. McWhan, IBM J. Res. Develop. 14, 251 (1970).

[10] J. B. Goodenough, in *Progress in Solid State Chemistry*, edited by H. Reiss (Pergamon, Oxford, 1971), Vol. 5, pp. 145ff.

[11] R. W. Vest and J. M. Honig, in *Electrical Conductivity of Ceramics*, edited by N. M. Tallan (Marcel Dekker, New York, to be published).

[12] C. S. Fadley, Lawrence Radiation Laboratory Report No. UCRL-19535, 1970 (unpublished).

[13] J. A. Bearden and A. F. Burr, Rev. Mod. Phys. 39, 125 (1967).

[14] D. W. Fischer, J. Appl. Phys. 40, 4151 (1969); 41, 3561 (1970).

[15] R. J. Powell, Stanford Electronics Laboratory Technical Report No. 5220-1, 1967 (unpublished).

[16] W. M. H. Sachtler, G. J. H. Dorgelo, and A. A. Holscher, Surface Sci. 5, 221 (1966).

[17] W. L. Jolly and D. N. Hendrickson, J. Am. Chem. Soc. 92, 1863 (1970).

[18] I. Nebenzahl and M. Weger, Phil. Mag. 24, 1119 (1971).

PHYSICAL REVIEW B VOLUME 6, NUMBER 4 15 AUGUST 1972

Photoelectronic Properties of Zinc Impurity in Silicon[†]

Alden F. Sklensky[*]
Department of Materials Science, Stanford University, Stanford, California 94305
and Lockheed Palo Alto Research Laboratories, Palo Alto, California 94304

and

Richard H. Bube
Department of Materials Science, Stanford University, Stanford, California 94305

(Received 23 February 1972)

Zinc impurity in high-resistivity *n*-type-silicon single crystals exhibits the properties of a sensitizing center for photoconductivity; the electron lifetime is increased by a factor of 10^4 to a value of 100 msec at 80 °K. A variety of photoelectronic measurements are used to determine the location of the Zn^{-2} energy level with respect to the conduction- and valence-band edges, the density of zinc centers, the change in scattering cross section upon photoexcitation, the electron-capture cross section of the Zn^{-1} center as a function of temperature, and the existence and properties of other imperfection states. Optical quenching of photoconductivity indicates an electron-capture cross section of the Zn^{-1} center which is about 10^{-20} cm^2 and independent of temperature below 50 °K, and which decreases exponentially with $1/T$ at higher temperatures with an activation energy of 40 meV. Measurements of temperature dependence of steady-state lifetime and of photoconductivity decay time are consistent.

INTRODUCTION

The photosensitivity of infrared detectors using II-VI or III-V compounds[1-6] is frequently enhanced several orders of magnitude by the presence of imperfections which behave as sensitizing centers and increase the free-electron lifetime. Sensitizing centers in II-VI and III-V compounds are generally assumed to be associated with intrinsic defects, but similar sensitizing imperfections associated with specific impurities are known in Ge and Si.[7-21] One of the most interesting of these is the case of Zn impurity in Si,[17-21] which provides an opportunity to investigate the properties of a known sensitizing center in a well-characterized material.

The saturation zinc concentration in silicon as a function of temperature and diffusivity has been established by Fuller and Morin[22] with some later refinements.[23-25] Fuller and Morin, and Carlson[26] report the existence of two acceptor levels associated with Zn as a double acceptor in Si; the possibility of a third acceptor level has been considered by other workers,[23] but its presence does not seem likely.[27,28] Values for the various cross sections associated with these two levels taken from the literature are summarized in Table I.

It was the purpose of the present investigation to explore the properties of Zn impurity in high-resistivity *n*-type-Si single crystals by the use of a variety of photoelectronic techniques. Of particular interest were the location of the Zn^{-2} energy level, the density of incorporated Zn centers, the scattering cross section associated with Zn impurity, the temperature dependence of the electron-capture cross section of the Zn^{-1} center, and the effects of other imperfections in the Si. The first four properties represent a rather complete characterization of the zinc sensitizing center in silicon and the temperature dependence of S_1^n provides information on the capture process of a Coulombically repulsive center.